

Research article

Enhanced nitrate removal by ternary electron donors of solid carbon source, pyrite, and iron-scrap in stormwater bioretention systems: Impact of natural and synthetic carbon sources



Zhaoying Liu ^{a,b}, Jiayu Li ^{a,b}, Jiaqi Zhang ^{a,b}, Yuanping Fang ^{a,b}, Haiyan Li ^{a,b,*}

^a Beijing Energy Conservation & Sustainable Urban and Rural Development Provincial and Ministry Co-construction Collaboration Innovation Center, Beijing University of Civil Engineering and Architecture, Beijing, 100044, China

^b Beijing Engineering Research Center of Sustainable Urban Sewage System Construction and Risk Control, Beijing University of Civil Engineering and Architecture, Beijing, 100044, China

ARTICLE INFO

Keywords:

Stormwater runoff
Bioretention systems
Electron donor
Mixotrophic denitrification
Microbial mechanisms

ABSTRACT

Insufficient availability of electron donors is challenging for nitrate removal in bioretention systems when treating carbon-limited stormwater runoff. This study constructed two ternary electron-donor systems incorporating solid carbon source, pyrite, and iron-scrap to enhance mixotrophic denitrification, and investigated the impacts of natural carbon source (woodchip) and synthetic carbon source (polycaprolactone) on denitrification performance and by-product generation. Results showed that both systems exhibited stable and efficient nitrate removal ($85.76 \pm 11.00\%$ and $89.67 \pm 5.75\%$) under 120 days of variable stormwater conditions, attributing to the synergy of multi-electron donors. Compared with the polycaprolactone-packed system, the woodchip-packed system showed substantial reductions in ammonia nitrogen, dissolved organic carbon, and sulfate production, indicating better comprehensive pollutant control. Woodchips avoided excessive corrosion and passivation of iron-scrap by maintaining low dissolved organic carbon conditions and preventing high OH^- production, and promoted the reduction of iron oxides through redox-active groups. Meanwhile, woodchips prevented the inhibition of autotrophic denitrification and released volatile fatty acids, stimulating pyrite bio-oxidation and sulfate reduction. The generated abundant free soluble iron and polysulfides immobilized each other and further enhanced autotrophic denitrification. The microbial community and PICRUSt2-based predicted functional analysis revealed that the woodchip-packed system enriched the heterotrophic denitrifiers, sulfur-oxidizing, sulfate-reducing, iron-oxidizing, and iron-reducing bacteria, along with the genes related to carbon, nitrogen, sulfur, iron metabolism, and electron transfer. The findings of this study demonstrated that coupling woodchips with pyrite and iron-scrap strengthened substrate cooperation and microbial synergy, offering a sustainable solution for efficient nitrate removal from stormwater runoff.

1. Introduction

Nitrate pollution poses a major global threat to aquatic ecosystems, driving eutrophication and biodiversity loss (Valenca et al., 2021; Yadav et al., 2024). Stormwater runoff, frequently discharged without adequate treatment, constitutes a significant source of nitrate pollution in receiving waters (Hou et al., 2023; Yadav et al., 2025). As the predominant nitrogen species in stormwater runoff, NO_3^- -N concentrations are strongly influenced by antecedent conditions and runoff characteristics, often peaking during initial rainfall (Wang et al., 2024b).

Bioretention systems represent effective nature-based solutions that harness synergistic interactions among plants, substrates, and microorganisms to mitigate runoff pollution (Ding et al., 2024; Jain et al., 2024). The creation of submerged zones with supplemental electron donors have become standard practice to address the lack of biodegradable organic matter in stormwater runoff for denitrification (Kong et al., 2021). Therefore, optimizing electron donor selection and combinations is crucial to improve electron donor availability and denitrification efficiency.

Previous research has investigated organic and inorganic substances

* Corresponding author. Beijing Energy Conservation & Sustainable Urban and Rural Development Provincial and Ministry Co-construction Collaboration Innovation Center, Beijing University of Civil Engineering and Architecture, Beijing, 100044, China.

E-mail address: lihaiyan@bucea.edu.cn (H. Li).

as single electron donors in bioretention systems to promote heterotrophic and autotrophic denitrification, respectively (Biswal et al., 2022). Yet, inconsistent efficiencies from initial operation through long-term application has hindered widespread adoption. Recently, combined organic and inorganic compounds has gained attention as dual electron donors for mixotrophic denitrification, demonstrating efficient nitrate removal, low by-product generation, and extended operational longevity in bioretention systems (Liu et al., 2023b). Pyrite (FeS_2), a highly abundant and widely distributed sulfide mineral, has been developed as an alternative electron donor. When coupled with multiple natural carbon sources (e.g., corn cobs, rice husks, woodchips), it enhances NO_3^- -N removal by 69.39 % under complex stormwater conditions (Chai et al., 2023). However, the key bottleneck of pyrite-driven mixotrophic denitrification is the poor electron availability due to the low solubility and dissolution rate of pyrite.

Coupling pyrite with Fe^0 can enhance the electron transport system activity, facilitate Fe (II)/ Fe (III) redox cycling, and increase the abundance of *Thiobacillus*, thereby improving the nitrate removal (Liu et al., 2023a). Additionally, pyrite can boost reactive Fe^{2+} production and prevent Fe^0 passivation through the galvanic couple formed by the potential difference between Fe^0 (-0.44 V) and FeS_2 (+0.35 V) (Lü et al., 2019). In sulfur autotrophic denitrification systems, iron-bearing compounds can additionally mitigate elevated acidity and sulfate generation (Wang et al., 2024c). Furthermore, mixotrophic denitrification coupling iron-scrap (Fe^0) with organic carbon sources can accelerate electron transfer by promoting extracellular polymeric substances (EPS) formation and enhance iron corrosion for biotransformation and storage (Wang et al., 2023). Integrating ternary electron donors of sulfur, iron, and organic carbon has been reported to improve reactor resistance and stability, while multi-media interaction can facilitate the protection and promotion between substrates (Kong et al., 2024; Lu et al., 2021). Multi-electron donors can improve microbial metabolism and denitrifying enzyme activity, facilitating the bio-utilization of sulfur-iron compounds (Zhang et al., 2025). Thus, using solid carbon sources, pyrite, and iron-scrap as substrates in bioretention systems could be an effective strategy to improve the efficiency and stability of nitrate removal. Nevertheless, synergistic interactions among ternary electron donors in bioretention systems under dynamic stormwater conditions remain unexplored, and the mechanisms driving the efficiency and stability of mixotrophic denitrification require further elucidation.

In addition, appropriate organic carbon sources are essential for synergism between heterotrophic and autotrophic microorganisms in mixotrophic denitrification systems, as carbon source type significantly influences denitrification efficiency. Solid carbon sources are broadly classified as natural or synthetic, differing in structure, hydrolysis capacity, hydrolysis products, carbon release patterns, denitrification performance, and cost (Zhang et al., 2021). Zhou et al. (2022) found that synthetic biodegradable polymers coupled with pyrite achieved superior denitrification performance (95.21 %) compared with natural biomass materials. Synthetic carbon sources offer higher mechanical properties and carbon release rates, whereas natural carbon sources often decompose rapidly resulting in unsustainable carbon release. Notably, decomposition products of natural carbon sources (humus containing rich quinone/hydroquinone moiety, soluble organic matter, and lignocellulose) can facilitate electron transfer to minerals and contribute to Fe^{2+} production, consequently enhancing both heterotrophic and autotrophic denitrification (Fan et al., 2024). However, the differential effects of natural versus synthetic carbon sources on substrate interactions, byproduct generation, and microbial synergies within ternary electron-donor systems remain unclear. Hence, it's necessary to better understand the role of different carbon sources in mixotrophic denitrification systems with ternary donors and the underlying mechanisms of carbon, nitrogen, sulfur, and iron metabolism involved in substrate coupling.

In this study, two bioretention systems were constructed by adding typical natural carbon sources (woodchips) and synthetic carbon sources

(polycaprolactone, PCL), respectively, coupled with pyrite and iron-scrap as functional substrates. The objectives were to (1) explore the impact of carbon source type on denitrification performance and by-product generation in ternary electron-donor systems, (2) investigate the characteristics and interactions among the three substrates, and (3) clarify the carbon, nitrogen, sulfur and iron metabolism mechanisms of microorganisms. The study aims to optimize electron donor combinations and improve the electron availability for mixotrophic denitrification, providing a potential strategy for efficient nitrate removal in bioretention systems.

2. Materials and methods

2.1. Design of bioretention systems

Two bioretention systems with submerged zones were constructed using cylindrical PVC material (20 cm diameter, 65 cm height, Fig. 1). Each system was divided from top to bottom into four layers: water storage layer, soil layer, media layer, and drainage layer (Table S1). The submerged zones maintaining anoxic conditions were created by raising the outlet by 35 cm. The media layers were filled with a mixture of quartz sand and ternary electron donor substrates (volume ratio of 9:1). The compositions of ternary electron donors in the two systems were woodchips, pyrite, and iron-scrap for WPI, and PCL, pyrite, and iron-scrap for PPI, both with a volume ratio of 2:1:1. Each system wrapped with tinfoil on the sides and equipped with several ports for water and solid sampling. *Iris lactea*, a typical plant in the "Sponge City" pilot area in Beijing, was selected as a soil layer plant, with strong drought and flooding tolerance. The height of *Iris lactea* was maintained at 400–500 mm in two systems, with a planting density of 15 plants/m².

2.2. Operation of bioretention systems

Both systems underwent microbial enrichment during the 15-day start-up (Stage I) using influent high in nutrients and trace elements. Continuous operation under variable stormwater conditions followed for 52 days (Stage II) and 53 days of stabilization (Stage III), with functional substrates and microbial samples collected in stage III. The synthetic wastewater for the formal operational stages was a simulation of initial stormwater runoff with high nitrate and low biodegradable organic matter levels, consisting of 10 mg/L of NO_3^- -N and 8 mg/L of DOC (McCabe et al., 2021; Wang et al., 2022). The NO_3^- -N concentration of 10 mg/L is consistent with the median to high values reported in urban stormwater studies and acceptable levels of the World Health Organization (Wang et al., 2024b), allowing for assessing the robustness of bioretention systems under actual pollution loads. In stage II, the effects of different rainfall intensities (35.03, 59.55, and 87.58 mm/h) and antecedent drying durations (3, 5, 7, 10, and 15 days) on system performance were investigated. The influent flow rates for low to high rainfall intensities were 8.33 mL/min, 31.17 mL/min, 45.83 mL/min, with corresponding hydraulic retention time (HRT) of 5.38 h, 3.17 h, and 2.15 h, respectively. The settings for influent volume and rainfall duration as well as the specific operational parameters for each stage are detailed in Text S1 and Table S2, respectively.

2.3. Sampling and analysis

2.3.1. Water sampling and analysis

Water samples from the influent and effluent of each system were collected according to the sampling frequency outlined in Table S2, and filtered through a 0.22 μm membrane filter for analysis of NO_3^- -N, NO_2^- -N, NH_4^+ -N, DOC, SO_4^{2-} , total iron (TFe), ORP and pH. The NO_3^- -N, NO_2^- -N, and SO_4^{2-} concentrations were determined using an ion chromatograph (881 Basic IC Plus, Metrohm, Switzerland). NH_4^+ -N concentration was measured with a UV-vis spectrophotometer (UV-6300, MAPADA, China). DOC concentration was detected by a total organic carbon

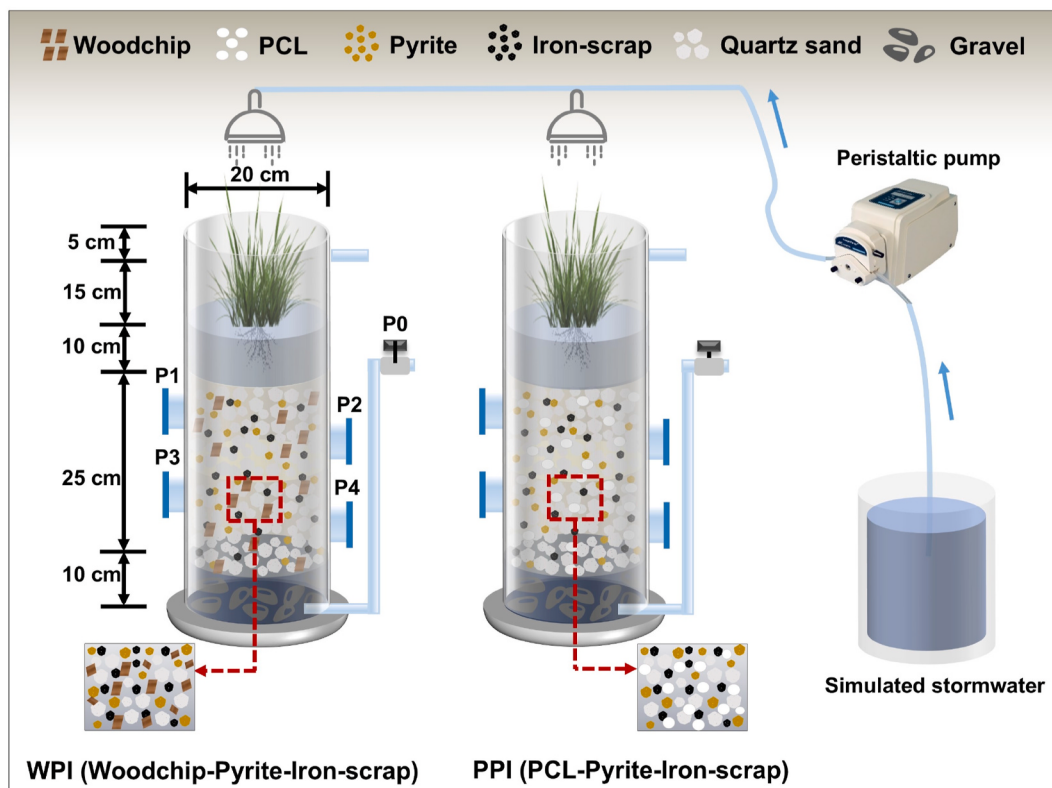


Fig. 1. Schematic diagram of WPI and PPI.

analyzer (TOC-LCSH, Shimadzu, Japan). TFe was analyzed by inductively coupled plasma optical emission spectroscopy (ICP-OES, PerkinElmer-Optima 8300, USA). ORP and pH values were measured with a multi-parameter water quality analyzer (Multi 3630, WTW, Germany) and benchtop instrument (STAR211, ThermoFisher Scientific, USA), respectively. All data were represented as the mean \pm standard deviation of three replicates. One-way analysis of variance (ANOVA) was performed using IBM SPSS Statistics 25, with results considered statistically significant at $p < 0.05$.

2.3.2. Substrates sampling and analysis

The used substrate samples (woodchips, PCL, pyrite, and iron-scrap) were collected from the media layer of each system at the end of stage III. The surface morphology of woodchips and PCL was observed using Scanning Electron Microscopy (SEM; FEI Quanta 250FEG, USA). Changes in the chemical composition and functional groups of solid carbon sources were examined using Fourier Transform Infrared Spectroscopy (FTIR; Thermo Fisher Scientific Nicolet iS5, USA). The elemental composition and valence of each substrate were analyzed using X-ray Photoelectron Spectroscopy (XPS; Thermo Fisher Scientific ESCALAB 250XI, USA).

2.3.3. Microbial community analysis

At the end of stage III, microbial samples (mixtures extracted from solid sampling ports P1-4) were collected from WPI and PPI to analyze microbial diversity and community composition through 16S rRNA high-throughput sequencing, as described in the detailed experimental procedures in Text S2. Functional genes associated with carbon, nitrogen, sulfur, and iron metabolism, as well as electron transfer, were predicted using PICRUSt2.

3. Results and discussion

3.1. Performance of two bioretention systems

3.1.1. Denitrification performance

Fig. 2a shows the variations in NO_3^- -N concentrations across three stages in two bioretention systems. Under the general conditions of influent NO_3^- -N concentration of 10 mg/L and total influent volume of 5.50 L per rainfall event, both WPI and PPI effectively removed NO_3^- -N throughout the period, with average removal efficiencies of $85.76 \pm 11.00\%$ and $89.67 \pm 5.75\%$, respectively. There was no significant difference in NO_3^- -N removal between systems in stages I and II ($p > 0.05$). During Stage I, characterized by high nitrate and organic matter levels, both systems rapidly achieved over 95% removal of NO_3^- -N by day 3, outperforming mono/dual electron-donor systems (took more than 14 days to initiate) in our previous study (Li et al., 2022). In stage II, under variable stormwater conditions, NO_3^- -N removal exhibited relatively minor fluctuations (80.35%–100%). This indicated that ternary substrates provided sufficient electron donors for denitrifying bacteria, promoting heterotrophic denitrification driven by woodchip/PCL (Eqs. (1)–(2)) and autotrophic denitrification driven by pyrite (Eq. (3)) and iron-scrap (Eqs. (4)–(5)) (Jin et al., 2019; Peng et al., 2021; Yuan et al., 2023). Additionally, abiotic reduction by iron-scrap (Eq. (6)) and dissimilatory nitrate reduction to ammonium (DNRA) driven by organic carbon, Fe^{2+} , and sulfide (S^{2-}) contributed to NO_3^- -N reduction to NH_4^+ -N (Pandey et al., 2020; Peng et al., 2021). The synergy of multiple reactions improved the stability of NO_3^- -N removal under complex stormwater conditions (Fig. S1) (Kong et al., 2024). Notably, PPI demonstrated better real-time NO_3^- -N removal (89.77–100%) versus WPI (63.90–100%) during rainfall (Fig. S1a), attributable to higher denitrification rate of PCL (1.23–3.80 g N/L•d) than woodchip (0.01–0.06 g N/L•d) (Pang and Wang, 2021). With continuous operation, NO_3^- -N removal efficiency significantly differed between the two systems in stage III ($p < 0.0001$). The average NO_3^- -N removal

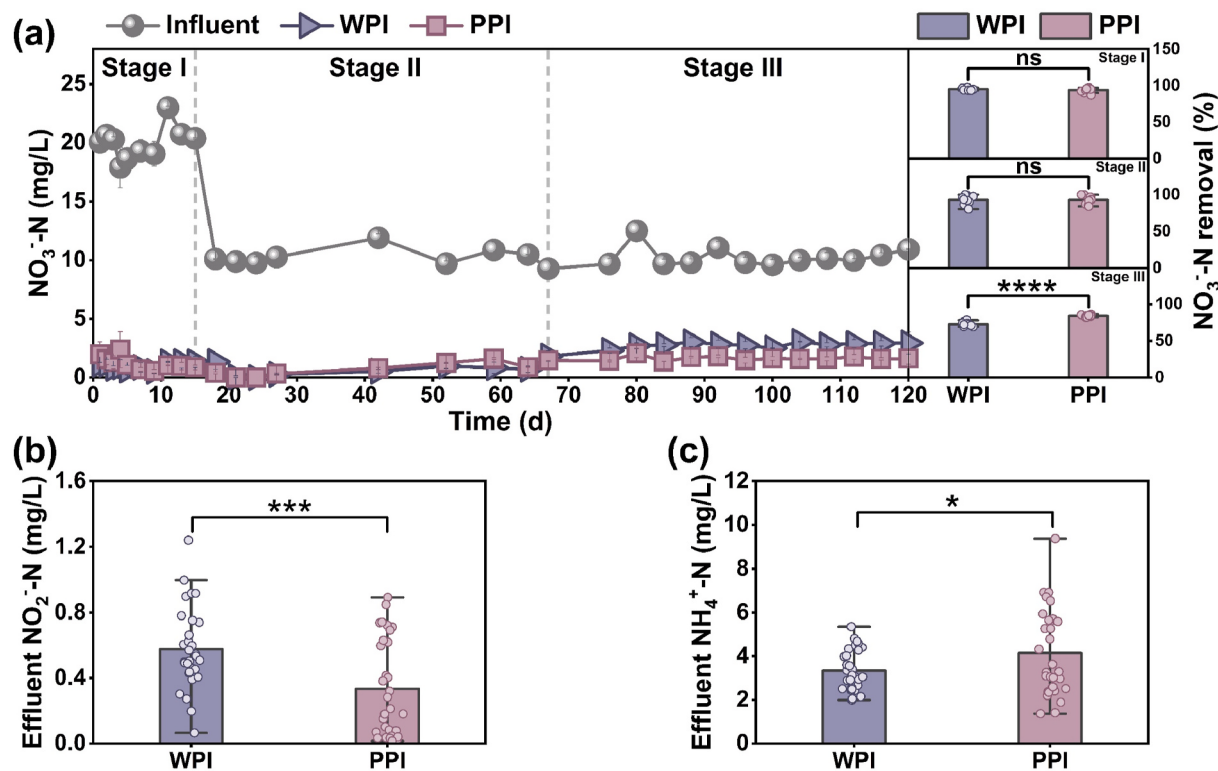
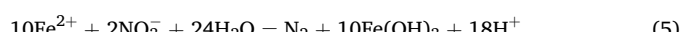
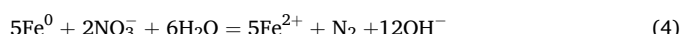
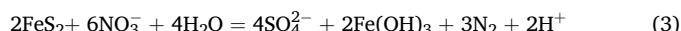
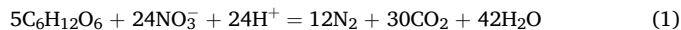


Fig. 2. Denitrification performances of WPI and PPI: (a) Influent and effluent NO₃⁻-N concentration and NO₃⁻-N removal efficiency. (b) Effluent NO₂⁻-N concentration. (c) Effluent NH₄⁺-N concentration.

efficiencies of WPI and PPI were $72.77 \pm 2.52\%$ and $84.07 \pm 1.15\%$, demonstrating improved long-term denitrification of PPI. This could be attributed to the greater sustainability of carbon release from synthetic biodegradable polymers than natural lignocellulosic materials (Zhang et al., 2021).



NO₂⁻-N, an intermediate product of both biotic (denitrification and DNRA) and abiotic (chemical reduction of Fe⁰) processes, accumulated less in PPI ($0.33 \pm 0.29\text{ mg/L}$) than in WPI ($0.58 \pm 0.24\text{ mg/L}$), particularly during later operational stages (Fig. 2b and Fig. S2a). This suggested that the coupling of PCL with pyrite and iron-scrap facilitated nitrate transformation completeness. NH₄⁺-N generation in both systems occurred through several possible pathways, including spontaneous nitrate reduction by Fe⁰, DNRA bioprocesses, and release by decaying microorganisms (Pipil et al., 2021; Shen et al., 2025). PPI ($4.14 \pm 1.95\text{ mg/L}$) generated more NH₄⁺-N than WPI ($3.34 \pm 0.91\text{ mg/L}$) (Fig. 2c), possibly due to the elevated organic carbon content promoting redox reactions mediated by Fe⁰ and the DNRA process (Pandey et al., 2020; Wang et al., 2023). As biological denitrification intensified in later operation, the effluent NH₄⁺-N concentrations from PPI decreased to below 2 mg/L (Fig. S2b). Excess NH₄⁺-N produced in the early stages could be further mitigated through establishing a bilayer structure in the submerged zone and incorporating adsorbents like zeolite (Liu et al., 2023b). This study focused on the interactions among ternary electron donors. On the whole, ternary electron donors significantly enhanced

NO₃⁻-N removal efficiency through the synergy of biotic and abiotic processes. PPI, utilizing synthetic carbon sources, provided sustained denitrification performance, but posed a potential risk of NH₄⁺-N leaching.

3.1.2. By-product generation

Organic by-products in WPI and PPI originated from solid carbon source release. The effluent DOC concentrations were consistently higher in PPI than WPI (Fig. 3a). During Stage I (influent DOC: $23.30 \pm 2.89\text{ mg/L}$), average effluent DOC measured $7.33 \pm 1.85\text{ mg/L}$ (WPI) and $11.45 \pm 2.67\text{ mg/L}$ (PPI). Elevated DOC levels stimulated heterotrophic denitrifying bacteria (Feng et al., 2023), but potentially enhanced DNRA process and accelerated iron transformation (Deng et al., 2020), contributing to increased NH₄⁺-N production. Initially, WPI demonstrated marginally superior NO₃⁻-N removal, likely due to abundant water-soluble small molecules on the surface and inside the woodchips that were readily bioavailable (Zhao et al., 2020). The effluent DOC concentration of WPI subsequently decreased to $6.13 \pm 4.71\text{ mg/L}$ during stages II and III. In later stages, the amount of carbon released from woodchips decreased but remained stable, and the proportion of remaining insoluble cellulose and hemicellulose was higher than small molecules, which slightly reduced denitrification performance. In contrast, PPI maintained higher DOC release ($11.42 \pm 4.87\text{ mg/L}$), primarily due to the substantial biodegradable polymers acting both as carbon sources and bacterial carriers, promoting microbial growth and metabolism (Zhang et al., 2021). Despite improved carbon availability over time, the potential risk of secondary pollution from carbon leaching during prolonged drying periods warrants attention (Fig. S1j).

SO₄²⁻ and TFe are typical by-products in systems using sulfur and iron compounds as substrates. SO₄²⁻ is mainly produced by sulfur autotrophic denitrification, sulfur disproportionation, and pyrite chemical oxidation by dissolved oxygen (DO) (Shen et al., 2025; Zhou et al., 2022). The effluent SO₄²⁻ concentrations of WPI and PPI were $21.40 \pm 7.80\text{ mg/L}$

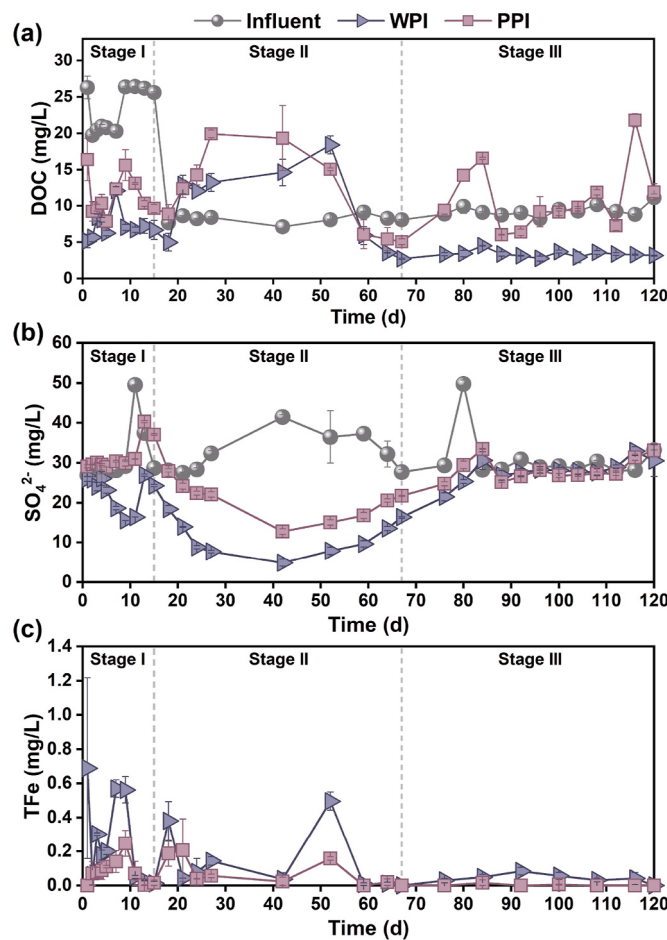


Fig. 3. By-product generation of WPI and PPI: (a) Influent and effluent DOC concentration. (b) Influent and effluent SO_4^{2-} concentration. (c) Effluent TFe concentration.

and $27.08 \pm 5.77 \text{ mg/L}$, respectively, below the influent level ($31.44 \pm 5.90 \text{ mg/L}$). This may be due to sulfate-reducing bacteria (SRB) utilizing organic matter as electron donors to reduce SO_4^{2-} to S^{2-} and S_n^{2-} (Parthipan et al., 2023). Sulfate reduction is a common phenomenon in mixotrophic denitrification systems, resulting in actual SO_4^{2-} production being much lower than the theoretical value (Pang et al., 2022). Both systems showed increased DOC and decreased SO_4^{2-} with longer antecedent drying durations (Fig. S1j-k). The sulfate reduction further enhanced by woodchips in WPI. Previous studies have indicated that natural carbon sources release more volatile fatty acids (VFA), which are more easily degraded by SRB (Bertolini et al., 2012; Feng et al., 2023).

The oxidation of pyrite and iron-scrap released Fe^{2+} and Fe^{3+} , providing electrons for NO_3^- -N reduction. The average effluent TFe concentration for PPI ($0.06 \pm 0.07 \text{ mg/L}$) was lower than that for WPI ($0.16 \pm 0.20 \text{ mg/L}$). Heterotrophic denitrification, promoted by PCL, released significant amounts of OH^- (Fig. S3a), which may have reacted with iron ions to form FeOOH precipitation, thereby covering the active sites on the surface of iron-scrap (Liu et al., 2018). The iron cycles mediated by pyrite and iron-scrap can enhance microbial metabolism, serve as electron donors, and participate in electron transfer (You et al., 2021), with varying effects depending on the type of organic carbon source (discussed in Section 3.2).

Overall, the combination of solid carbon sources, pyrite, and iron-scrap worked effectively in bioretention systems. However, natural versus synthetic carbon sources yielded distinct by-products despite efficient nitrate removal. According to the comprehensive pollution index calculation (Text S3), the index for WPI was lower than for PPI

(Table S3), suggesting that natural carbon sources better-mitigated pollution transfer during denitrification.

3.2. Changes of substrates characteristic

3.2.1. Solid carbon source

To investigate the substrate interaction mechanisms in ternary electron-donor systems, SEM, FTIR, and XPS were employed for the characterization of used substrates. Fig. 4a shows the surface morphology of raw and used woodchips and PCL. The raw woodchips exhibited a distinct fibrous surface, while the used woodchips in WPI displayed a rough, porous surface due to soaking and scouring during dry-wet cycles (Weng et al., 2022). Although this structural change facilitated microbial attachment, it likely reduced the availability of released organic carbon. The remaining fibrous structure, consisting mainly of cellulose and lignin, was resistant to decomposition (Fan et al., 2024). Conversely, PCL maintained surface roughness conducive to biofilm formation without significant structural alteration, underscoring its stability for sustained carbon release. FTIR analysis revealed significant reductions in wave peaks for the used woodchips (Fig. 4b), with the disappearance of C-O absorption peaks, suggesting macromolecular ring structure degradation during extended operation (Xiong et al., 2020). PCL exhibited more complex spectra than woodchip, but no significant changes in the characteristic peaks after use, confirming structural stability. The emergent weak O-H peak may stem from hydroxyl-containing metabolites generated during PCL hydrolytic degradation (Li et al., 2024). The O1s XPS spectra were employed to analyze the changes in oxygen-containing functional groups on the surface of solid carbon sources (Fig. 4c). For used woodchips, the peak intensities of O-C=O/-OH and C-O-C/C-OH decreased, while C=O and -COOH peak intensities increased. The extensive formation of electron-accepting moieties demonstrated a notable decrease in the electron supply and transfer capacity after prolonged operation. However, this may also have led to the exposure of more reactive molecules involved in the redox cycle (Fan et al., 2024), facilitating the cycling of iron. The increase in the O-C=O/-OH peak and decrease in C-O-C/C-OH for used PCL suggested the formation of alcohols from ester bond breakdown. Previous studies have reported that minimal PCL chemical alteration from hydrolysis and biological utilization (Zhang et al., 2016).

3.2.2. Iron-scrap

The valence states of iron in iron-scrap were characterized using XPS (Fig. 4d). The Fe 2p XPS spectra revealed a higher Fe (III)/Fe (II) ratio in PPI (0.47) than in WPI (0.36). The increased relative content of Fe (III) suggested that PCL accelerated the corrosion of iron-scrap, facilitating the Fe (II)-Fe (III) conversion and reducing the ORP of the submerged zone (Fig. S3b). Studies have shown that high doses of organic carbon can effectively promote Fe^0 corrosion, enhancing both biological and chemical nitrate transformation (Deng et al., 2020). While providing sufficient electrons for nitrate reduction, this simultaneously increased NH_4^+ -N generation in PPI. The presence of OH^- confirmed that extensive iron oxidation to FeOOH under high pH conditions in PPI, leading to a decrease in free iron (Fig. S4). Therefore, the high carbon release from PCL concurrently promoted the corrosion and passivation of iron-scrap, ultimately inhibiting electron donation (You et al., 2017). In comparison, woodchips in WPI mitigated iron-scrap surface passivation, enabling sustained electron accommodation. Redox-active groups formed on woodchip surfaces potentially facilitated the reduction of iron oxides, yielding more bioavailable iron. Released Fe^{2+} and Fe^{3+} enhanced biological enzyme activity and supported both heterotrophic and autotrophic microorganism growth (Bassin et al., 2016).

3.2.3. Pyrite

The XPS Fe2p and S2p spectra further revealed differences in the oxidation degree of pyrite between the two systems. For the used pyrite in WPI and PPI, the Fe (III) contents were 21.10 % and 16.07 %, the Fe

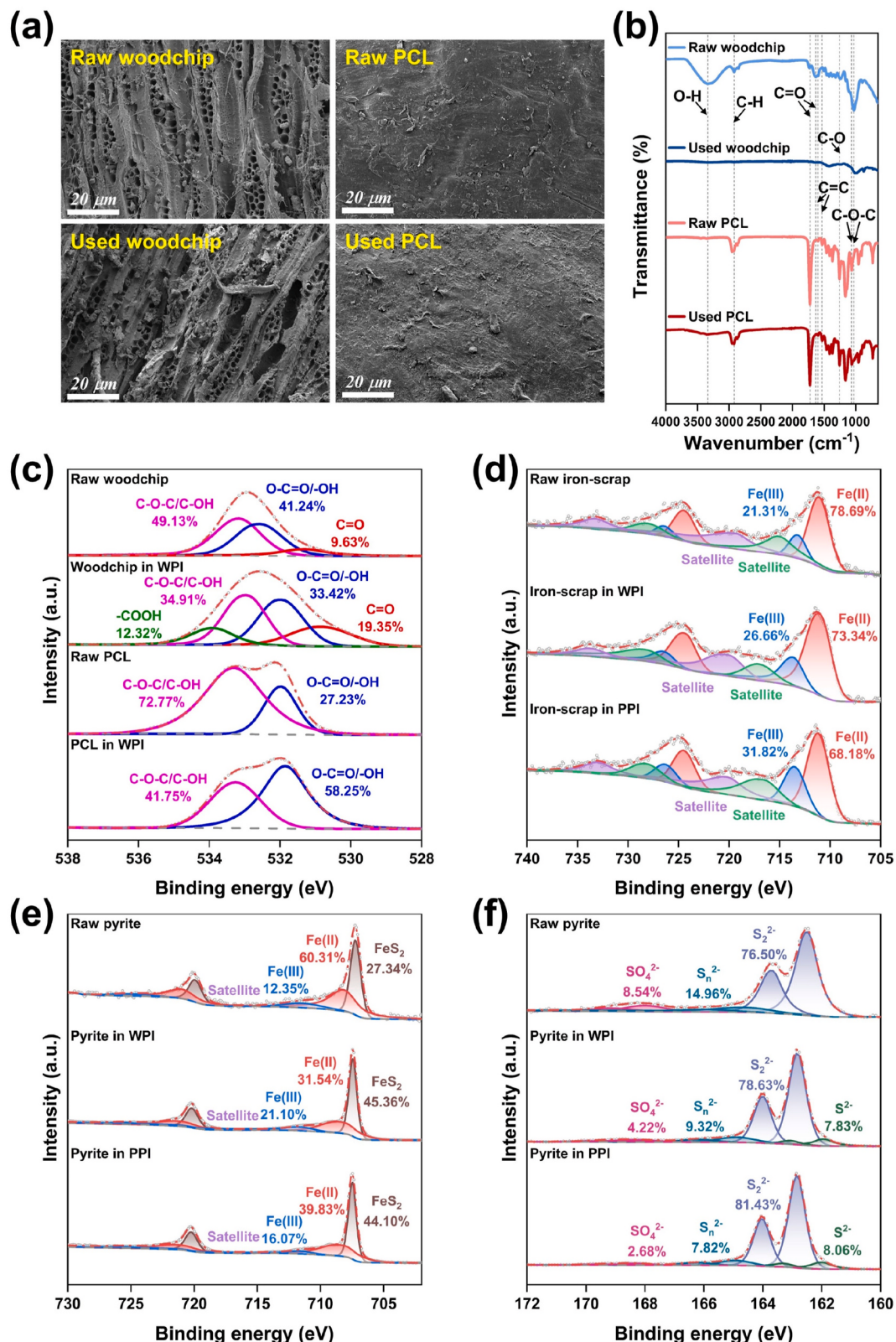


Fig. 4. Characteristic changes of substrates in WPI and PPI: (a) SEM images and (b) FTIR spectra of raw/used woodchip and raw/used PCL, (c) XPS spectral peaks of O1s of raw/used woodchip and raw/used PCL, (d) XPS spectral peaks of Fe2p of raw/used iron-scrap, and XPS spectral peaks of (e) Fe2p and (f) S2p of raw/used pyrite.

(II) contents were 31.54 % and 39.83 %, and the Fe(III)/Fe(II) ratios were 0.67 and 0.43, respectively (Fig. 4e). This indicated that woodchips facilitated the oxidation of Fe (II) to Fe (III). The low DOC release in WPI reduced the contribution of heterotrophic denitrification to nitrate removal, avoiding the limitation of Fe (III) production by autotrophic denitrification. Notably, FeS_2 content was significantly higher in WPI, likely due to sulfate reduction. Yang et al. (2024) proposed that organic-rich submerged zones can enrich SRB, which produces sulfide that can react with $\text{Fe}^{2+}/\text{Fe}^{3+}$ to form Fe_2S_3 , FeS , and more stable FeS_2 , promoting chemolithotrophic denitrification. Woodchips can release more low molecular weight compounds that support SRB growth while preventing high enrichment of heterotrophic denitrifying bacteria that compete with SRB (Wang et al., 2024c). Additionally, sulfate reduction requires H^+ utilization (Fuess et al., 2023), and the enhancement of autotrophic denitrification in WPI provided sufficient H^+ to maintain a favorable pH for the equilibrium between heterotrophic denitrification, autotrophic denitrification, and sulfate reduction (Fig. S3a). Therefore, as shown in Fig. 4f, the contents of S_2^{2-} and S^{2-} were lower, SO_4^{2-} was higher, and Sn^{2+} , an intermediate product of sulfate reduction and pyrite oxidation, was higher in WPI with respect to PPI. The complex sulfur cycle in WPI possibly immobilized more dissolved iron from iron-scrap into sulfur-iron species rather than FeOOH . In summary, despite limited sustained carbon release, woodchips demonstrated superior cooperative capacity with other electron donors, enhancing the activity of pyrite and iron-scrap and facilitating the cycling of sulfur and iron. These findings demonstrate that adequate carbon sources can fully exploit the synergy of ternary electron donors to promote denitrification while minimizing by-product generation. Natural carbon sources exhibited a stronger “substrate-protect-promote” effect than synthetic carbon sources in the ternary electron-donor systems, highlighting their role in maintaining the continuous electron supply capacity.

3.3. Microbial analysis

3.3.1. Microbial diversity and community composition

To assess the impact of natural and synthetic carbon sources on microbial communities in ternary electron donor systems, microbial diversity and community composition were revealed by high-throughput sequencing analyses. Table S4 presents the alpha diversity indices, showing that both systems had coverage values exceeding 99 %, indicating reliable results. WPI displayed higher richness (Chao 1 and ACE) and Shannon diversity than PPI, suggesting that woodchips improved the richness and diversity of the microbial community compared with PCL. Enhanced microbial diversity may improve the adaptability and stability of bioreactors (Yang et al., 2020).

At the phylum level, microbial community composition was similar between systems (Fig. 5a). The dominant bacteria were Proteobacteria (66.36 %–68.83 %), Firmicutes (11.89 %–13.39 %), Bacteroidetes (7.10 %–7.42 %), Patescibacteria (2.85 %–5.82 %), and Actinobacteria (2.76 %–4.64 %). Proteobacteria, abundant in bioreactors for wastewater treatment, contain most heterotrophic and autotrophic denitrifiers (Zhang et al., 2022). Bacteroidetes is the major phylum involved in the hydrolysis of high molecular weight organic compounds to support heterotrophic denitrification, accounting for a relatively high proportion of PPI (Wang et al., 2021).

At the genus level, microbial communities varied notably with the type of carbon sources (Fig. 5b). In PPI, *Diaphorobacter* and *Simplicispira* were more abundant, comprising 27.79 % and 13.99 %, respectively. These genera are known for metabolizing macromolecular polymers in PCL-packed reactors to promote heterotrophic denitrification (He et al., 2021). In contrast, WPI exhibited a lower abundance of heterotrophic denitrifying bacteria, including *Rhodocyclaceae_unclassified* (11.49 %), *Thauera* (7.41 %), *Prolixibacteraceae_uncultured* (5.95 %), and *Trichococcus* (5.78 %), which are involved in nitrogen transformation and aromatic compound degradation (Chen et al., 2023b; Shi et al., 2022; Sun et al., 2021; Tao et al., 2022). The abundance of autotrophic

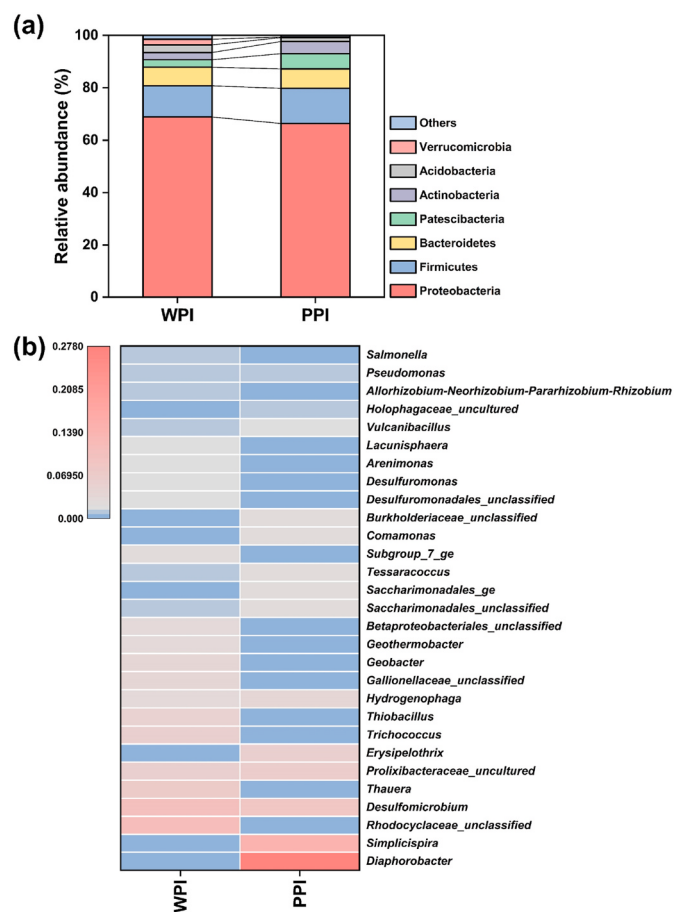


Fig. 5. Microbial community compositions of samples in WPI and PPI at (a) phylum level and at (b) genus level (relative abundance >1 % in at least one sample).

denitrifiers, particularly *Thiobacillus*, was significantly higher in WPI (5.49 %) than in PPI (0.02 %). *Thiobacillus* can reduce nitrate anaerobically using sulfur, sulfide, and divalent iron as electron donors (Chen et al., 2023a). In addition, SRB (*Desulfomicrobium*, *Desulfuromonas*, and *Geothermobacter*), iron-oxidizing bacteria (*Gallionellaceae_unclassified*), iron-reducing bacteria (*Geobacter*), and DNRA bacteria (*Lacunisphaera* and *Geobacter*) were more abundant in WPI (24.56 %) than in PPI (9.55 %) (Pang et al., 2021; Parthipan et al., 2023; Shi et al., 2022; Wang et al., 2020). This demonstrated that more complex synergistic interactions in the woodchip-pyrite-iron-scrap systems, support active electron transfer and cycling of carbon, nitrogen, sulfur, and iron. Notably, *Hydrogenophaga*, utilizing hydrogen from iron corrosion for hydrogenotrophic denitrification, was enriched in PPI (4.14 %), reflecting the higher corrosion rate of iron-scrap in PPI (Liu et al., 2020). These results highlight biological factors contributing to distinct contaminant transformation and substrate changes between the two systems.

3.3.2. Microbial functional metabolism

Fig. 6 shows the distribution and relative abundance of functional genes involved in carbon, nitrogen, and sulfur metabolism based on PICRUSt2 predictions in WPI and PPI. As both systems were dominated by heterotrophic denitrification, microbial metabolism depended on carbon degradation pathways including glycolytic and tricarboxylic acid cycle (TCA) to generate electrons and ATP (Zhang et al., 2024). Significant differences in carbon degradation gene abundances were observed between systems (Fig. 6a). WPI exhibited higher relative abundance of key enzymes in glycolysis especially aldehyde-3-phosphate dehydrogenase (*gapA*), indicating enhanced degradation of low molecular weight

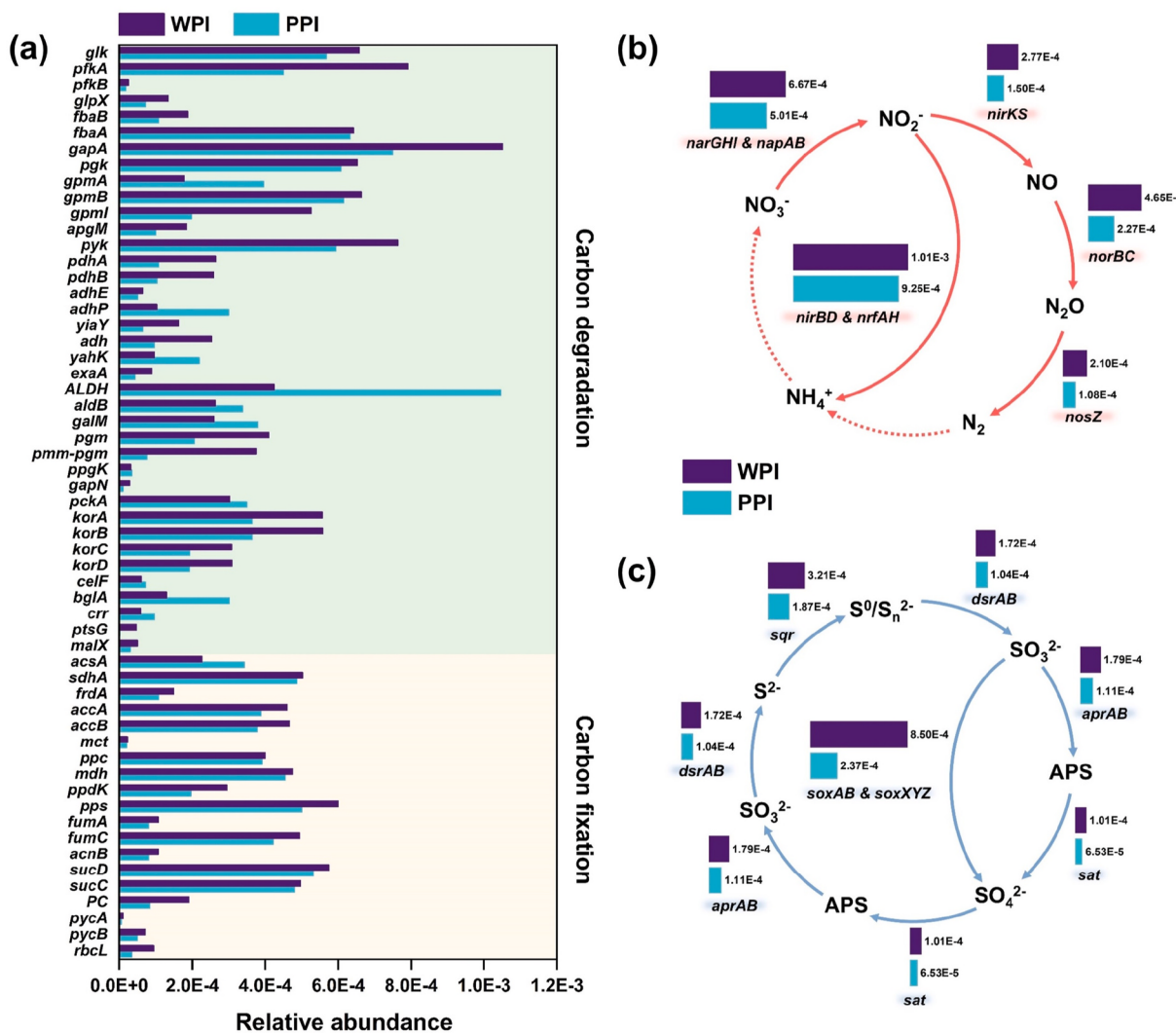


Fig. 6. Relative abundance of genes in WPI and PPI: (a) Carbon metabolism, (b) Nitrogen metabolism, and (c) Sulfur metabolism.

carbohydrates (Hao et al., 2024). Conversely, PPI showed upregulated genes associated with fatty acid metabolism (*ALDH* and *aldB*), reflecting PCL's distinct degradation pathways. Furthermore, WPI contained elevated abundances of carbon fixation genes, suggesting greater auto-trophic activity where sulfur and iron species serve as electron donors for converting inorganic carbon to organic compounds.

Regarding nitrogen metabolism, WPI possessed higher relative abundances of denitrification genes (*narGHI*, *napAB*, *nirKS*, *norBC*, *nosZ*), indicating more active complete nitrate reduction to N₂ (Fig. 6b). This contrasts with PPI, where increased nitrate removal primarily resulted from enhanced chemical reduction by Fe⁰, yielding higher ammonium production. The synergy between heterotrophic and auto-trophic denitrification in WPI contributed to more complete nitrate removal with reduced greenhouse gas emissions. Additionally, WPI showed higher abundances of DNRA genes (*nirBD*, *nrfAH*), potentially due to S²⁻ availability as electron donors for DNRA microorganisms (Wang et al., 2024a).

As for sulfur metabolism, WPI displayed significantly increased abundances of sulfur oxidation (*sqr* and *soxAB* & *soxXYZ*) and sulfate reduction (*aprAB* and *dsrAB*) genes (Fig. 6c). This indicated that the coupling of woodchips and pyrite enhanced the activity of sulfur auto-trophic denitrifying bacteria and SRB, facilitating the sulfur cycle and supporting the sustained utilization of pyrite. Fig. S5 presents the functional genes associated with the iron cycle in both systems. PPI was enriched in genes encoding iron complex outer-membrane receptor

proteins (*TC.FEV.OM*) and iron complex transporters (*ABC.FEV* and *afluABC*), which have been reported to be upregulated with increasing C/N ratios (Xiang et al., 2025). The rapid corrosion and passivation of iron-scrap generated abundant iron-containing compounds, which critically relied on these key enzymes to promote iron cycling (Guo et al., 2024). In contrast, WPI increased abundances of transporter proteins (*feoBC*) and ferredoxin oxidoreductases (*korBC*), which transport and oxidize Fe²⁺ to provide electrons. Consequently, woodchips enhanced the activity of pyrite and iron-scrap, continuously releasing soluble Fe²⁺ to stimulate iron-mediated denitrification. Fig. S6 further shows higher abundances of electron transfer genes in WPI, particularly *menCE* and *ribA*, which are involved in electron shuttle synthesis. These results demonstrated that coupling woodchips with pyrite and iron-scrap improved electron transfer between microorganisms and substrates, enhancing overall carbon, nitrogen, sulfur, and iron metabolism.

4. Conclusion

This study developed a novel ternary electron-donor bioretention system incorporating solid carbon sources, pyrite, and iron-scrap, and examined the impact of natural versus synthetic carbon sources. The woodchip-pyrite-iron-scrap system (WPI) demonstrated improved by-product control while efficiently denitrifying compared with the PCL-pyrite-iron-scrap system (PPI). Woodchips mitigated the negative effects of iron-scrap passivation and promoted the bio-utilization of pyrite,

showing an effective synergistic interaction with pyrite and iron-scrap for the collaboration of heterotrophic and autotrophic bacteria. Functional genes related to carbon fixation, denitrification, sulfur oxidation, sulfate reduction, ferric ion transfer, and electron transfer were significantly more abundant in WPI, highlighting the boosted cycling of carbon, nitrogen, sulfur, and iron. The synergistic interactions among the three electron donors strengthened substrates activity and extended system lifespan, providing new insights into optimizing electron donors for improved nitrate removal in bioretention systems. In practical construction of bioretention systems, ternary composite substrates can be uniformly blended and embedded within the media layer to treat urban catchment runoff with high nitrate loads. The organic-to-inorganic substrate ratio may be adjusted based on the biodegradable organic matter concentration in stormwater runoff, thereby enhancing substrate utilization efficiency. Considering the advantages and roles of each electron donor, future work should focus on the development of novel slow-release composites while optimizing the ratio and content of ternary electron donors to further improve overall pollution control capacity.

CRediT authorship contribution statement

Zhaoying Liu: Writing – original draft, Methodology, Investigation, Data curation. **Jiayu Li:** Formal analysis, Data curation. **Jiaqi Zhang:** Investigation, Data curation. **Yuaping Fang:** Writing – review & editing, Formal analysis. **Haiyan Li:** Supervision, Resources, Funding acquisition, Conceptualization.

Declaration of competing interest

The authors declare that they have no known competing financial interests or personal relationships that could have appeared to influence the work reported in this paper.

Acknowledgments

This work was supported by the National Natural Science Foundation of China (No. 52270086), the Youth Beijing Scholars program (No. 024), Beijing Natural Science Foundation (No.8252024, No.8254053), the Cultivation project Funds for Beijing University of Civil Engineering and Architecture (X24028), and the BUCEA Doctor Graduate Scientific Research Ability Improvement Project (DG2024024).

Appendix A. Supplementary data

Supplementary data to this article can be found online at <https://doi.org/10.1016/j.jenvman.2025.126646>.

Data availability

Data will be made available on request.

References

- Bassin, J.P., Dias, I.N., Cao, S.M.S., Senra, E., Laranjeira, Y., Dezotti, M., 2016. Effect of increasing organic loading rates on the performance of moving-bed biofilm reactors filled with different support media: assessing the activity of suspended and attached biomass fractions. Process. Saf. Environ. 100, 131–141. <https://doi.org/10.1016/j.psep.2016.01.007>.
- Bertolini, S.M., Rodrigues, I.C.B., Guerra-Sá, R., Aquino, S.F., Leão, V.A., 2012. Implications of volatile fatty acid profile on the metabolic pathway during continuous sulfate reduction. J. Environ. Manag. 103, 15–23. <https://doi.org/10.1016/j.jenvman.2012.02.022>.
- Biswal, B.K., Vijayaraghavan, K., Adam, M.G., Lee Tsen-Tieng, D., Davis, A.P., Balasubramanian, R., 2022. Biological nitrogen removal from stormwater in bioretention cells: a critical review. Crit. Rev. Biotechnol. 42 (5), 713–735. <https://doi.org/10.1080/07388551.2021.1969888>.
- Chai, H., Ma, J., Ma, H., Cheng, H., Weng, Z., Kong, Z., Shao, Z., Yuan, Y., Xu, Y., Ni, Q., Li, L., 2023. Enhanced nutrient removal of agricultural waste-pyrite bioretention system for stormwater pollution treatment. J. Clean. Prod. 395, 136457. <https://doi.org/10.1016/j.jclepro.2023.136457>.
- Chen, Z., Pang, C., Wen, Q., 2023a. Coupled pyrite and sulfur autotrophic denitrification for simultaneous removal of nitrogen and phosphorus from secondary effluent: feasibility, performance and mechanisms. Water Res. 243, 120422. <https://doi.org/10.1016/j.watres.2023.120422>.
- Chen, Z., Zuo, Q., Liu, C., Li, L., Deliz Quinones, K.Y., He, Q., 2023b. Insights into solid phase denitrification in wastewater tertiary treatment: the role of solid carbon source in carbon biodegradation and heterotrophic denitrification. Bioresour. Technol. 376, 128838. <https://doi.org/10.1016/j.biortech.2023.128838>.
- Deng, S., Peng, S., Xie, B., Yang, X., Sun, S., Yao, H., Li, D., 2020. Influence characteristics and mechanism of organic carbon on denitrification, N₂O emission and NO₂ accumulation in the iron [Fe(0)]-oxidizing supported autotrophic denitrification process. Chem. Eng. J. 393, 124736. <https://doi.org/10.1016/j.cej.2020.124736>.
- Ding, W., Qin, H., Wang, F., Xia, C., 2024. Leaching sources and mechanisms of different nitrogen species from bioretention systems. Water Res. 260, 121911. <https://doi.org/10.1016/j.watres.2024.121911>.
- Fan, Y., Sun, S., Gu, X., Zhang, M., Peng, Y., Yan, P., He, S., 2024. Boosting the denitrification efficiency of iron-based constructed wetlands in-situ via plant biomass-derived biochar: intensified iron redox cycle and microbial responses. Water Res. 253, 121285. <https://doi.org/10.1016/j.watres.2024.121285>.
- Feng, Y., Wang, L., Yin, Z., Cui, Z., Qu, K., Wang, D., Wang, Z., Zhu, S., Cui, H., 2023. Comparative investigation on heterotrophic denitrification driven by different biodegradable polymers for nitrate removal in mariculture wastewater: organic carbon release, denitrification performance, and microbial community. Front. Microbiol. 14 (1), 1141362. <https://doi.org/10.3389/fmicb.2023.1141362>.
- Fuess, L.T., Braga, A.F.M., Eng, F., Gregoracci, G.B., Saia, F.T., Zaiat, M., Lens, P.N.L., 2023. Solving the bottlenecks of sugarcane vinasse biodigestion: impacts of temperature and substrate exchange on sulfate removal during dark fermentation. Chem. Eng. J. 455, 140965. <https://doi.org/10.1016/j.cej.2022.140965>.
- Guo, H., Li, N., Xue, S., Zhangsun, X., Huang, T., Zhang, H., Ma, B., 2024. Enhancing nitrogen removal in source water with intermittent aeration: improved performance of iron-reducing denitrifying bacteria. Chem. Eng. J. 498, 154960. <https://doi.org/10.1016/j.cej.2024.154960>.
- Hao, Q., Lyu, X., Qin, D., Du, N., Wu, S., Bai, S., Chen, Z., Wang, P., Zhao, X., 2024. Synergistic mechanisms of denitrification in FeS₂-based constructed wetlands: effects of organic carbon availability under day-night alterations. Bioresour. Technol. 406, 131066. <https://doi.org/10.1016/j.biortech.2024.131066>.
- He, X., Zhang, S., Jiang, Y., Li, M., Yuan, J., Wang, G., 2021. Influence mechanism of filling ratio on solid-phase denitrification with polycaprolactone as biofilm carrier. Bioresour. Technol. 337, 125401. <https://doi.org/10.1016/j.biortech.2021.125401>.
- Hou, Y., Wang, S., Ma, Y., Shen, Z., Goonetilleke, A., 2023. Influence of landscape patterns on nitrate and particulate organic nitrogen inputs to urban stormwater runoff. J. Environ. Manag. 348, 119190. <https://doi.org/10.1016/j.jenvman.2023.119190>.
- Jain, N., Yadav, S., Taneja, S., Ray, S., Haritash, A.K., Pipil, H., 2024. Phosphate removal from urban stormwater runoff using *Canna lily* and *Cyperus alternifolius*-based bioretention system. Sustain. Water Resour. Manag. 10, 65. <https://doi.org/10.1007/s40899-024-01076-5>.
- Jin, S., Feng, C., Tong, S., Chen, N., Liu, H., Zhao, J., 2019. Effect of sawdust dosage and hydraulic retention time (HRT) on nitrate removal in sawdust/pyrite mixotrophic denitrification (SPMD) systems. Environ. Sci. Water Res. Technol. 5 (2), 346–357. <https://doi.org/10.1039/C8EW00748A>.
- Kong, Z., Song, Y., Shao, Z., Chai, H., 2021. Biochar-pyrite bi-layer bioretention system for dissolved nutrient treatment and by-product generation control under various stormwater conditions. Water Res. 206, 117737. <https://doi.org/10.1016/j.watres.2021.117737>.
- Kong, Z., Song, Y., Xu, M., Yang, Y., Wang, X., Ma, H., Zhi, Y., Shao, Z., Chen, L., Yuan, Y., Liu, F., Xu, Y., Ni, Q., Hu, S., Chai, H., 2024. Multi-media interaction improves the efficiency and stability of the bioretention system for stormwater runoff treatment. Water Res. 250, 121017. <https://doi.org/10.1016/j.watres.2023.121017>.
- Li, H., Liu, Z., Tan, C., Zhang, X., Zhang, Z., Bai, X., Wu, L., Yang, H., 2022. Efficient nitrogen removal from stormwater runoff by bioretention system: the construction of plant carbon source-based heterotrophic and sulfur autotrophic denitrification process. Bioresour. Technol. 349, 126803.
- Li, Z., Huang, T., Wu, W., Xu, X., Wu, B., Zhuang, J., Yang, J., Shi, H., Zhang, Y., Wang, B., 2024. Carbon slow-release and enhanced nitrogen removal performance of plant residue-based composite filler and ecological mechanisms in constructed wetland application. Bioresour. Technol. 402, 130795. <https://doi.org/10.1016/j.biortech.2022.126803>.
- Li, H., Chen, Z., Guan, Y., Xu, S., 2018. Role and application of iron in water treatment for nitrogen removal: a review. Chemosphere 204, 51–62. <https://doi.org/10.1016/j.chemosphere.2018.04.019>.
- Liu, X., Huang, M., Bao, S., Tang, W., Fang, T., 2020. Nitrate removal from low carbon-to-nitrogen ratio wastewater by combining iron-based chemical reduction and autotrophic denitrification. Bioresour. Technol. 301, 122731. <https://doi.org/10.1016/j.biortech.2019.122731>.
- Liu, X., Xin, X., Yang, W., Zhang, X., 2023a. Effect mechanism of micron-scale zero-valent iron enhanced pyrite-driven denitrification biofilter for nitrogen and phosphorus removal. Bioproc. Biosyst. Eng. 46 (12), 1847–1860. <https://doi.org/10.1007/s00449-023-02941-x>.
- Liu, Z., Wu, L., Hao, Y., Cheng, Y., Tan, C., Wang, J., Li, H., 2023b. Nitrogen removal performance and C, N, S transformation under dry-wet alterations of heterotrophic-

- autotrophic sequential bioretention system amended with waste reed and sulfur. *J. Clean. Prod.* 426, 139167. <https://doi.org/10.1016/j.jclepro.2023.139167>.
- Lu, X., Wan, Y., Zhong, Z., Liu, B., Zan, F., Zhang, F., Wu, X., 2021. Integrating sulfur, iron(II), and fixed organic carbon for mixotrophic denitrification in a composite filter bed reactor for decentralized wastewater treatment: performance and microbial community. *Sci. Total Environ.* 795, 148825. <https://doi.org/10.1016/j.scitotenv.2021.148825>.
- Lü, Y., Li, J., Li, Y., Liang, L., Dong, H., Chen, K., Yao, C., Li, Z., Li, J., Guan, X., 2019. The roles of pyrite for enhancing reductive removal of nitrobenzene by zero-valent iron. *Appl. Catal. B Environ.* 242, 9–18. <https://doi.org/10.1016/j.apcatb.2018.09.086>.
- McCabe, K.M., Smith, E.M., Lang, S.Q., Osburn, C.L., Benitez-Nelson, C.R., 2021. Particulate and dissolved organic matter in stormwater runoff influences oxygen demand in urbanized headwater catchments. *Environ. Sci. Technol.* 55 (2), 952–961. <https://doi.org/10.1021/acs.est.0c04502>.
- Pandey, C.B., Kumar, U., Kaviraj, M., Minick, K.J., Mishra, A.K., Singh, J.S., 2020. DNRA: a short-circuit in biological N-cycling to conserve nitrogen in terrestrial ecosystems. *Sci. Total Environ.* 738, 139710. <https://doi.org/10.1016/j.scitotenv.2020.139710>.
- Pang, Y., Hu, L., Wang, J., 2022. Mixotrophic denitrification using pyrite and biodegradable polymer composite as electron donors. *Bioresour. Technol.* 351, 127011. <https://doi.org/10.1016/j.biortech.2022.127011>.
- Pang, Y., Wang, J., 2021. Various electron donors for biological nitrate removal: a review. *Sci. Total Environ.* 794, 148699. <https://doi.org/10.1016/j.scitotenv.2021.148699>.
- Pang, Y., Wang, J., Li, S., Ji, G., 2021. Long-term sulfide input enhances chemoaerotrophic denitrification rather than DNRA in freshwater lake sediments. *Environ. Pollut.* 270, 116201. <https://doi.org/10.1016/j.envpol.2020.116201>.
- Parthipan, P., Cheng, L., Dhandapani, P., Rajasekar, A., 2023. Metagenomics diversity analysis of sulfate-reducing bacteria and their impact on biocorrosion and mitigation approach using an organometallic inhibitor. *Sci. Total Environ.* 856 (Pt 2), 159203. <https://doi.org/10.1016/j.scitotenv.2022.159203>.
- Peng, Y., He, S., Wu, F., 2021. Biochemical processes mediated by iron-based materials in water treatment: enhancing nitrogen and phosphorus removal in low C/N ratio wastewater. *Sci. Total Environ.* 775, 145137. <https://doi.org/10.1016/j.scitotenv.2021.145137>.
- Pipil, H., Haritash, A.K., Reddy, K.R., 2021. Seasonal variability and kinetics of phosphate removal in a phragmites-based engineered wetland. *Rend. Fis. Acc. Lincei.* 32, 729–735. <https://doi.org/10.1007/s12210-021-01017-w>.
- Shen, Y., Zhao, G., Wan, D., Liu, M., Peng, T., Zhang, W., Wang, P., He, Q., 2025. Dual-layer elemental sulfur-packed denitrification reactor to control sulfate generation and sulfide discharge by two-point inlet and internal recirculation. *Bioresour. Technol.* 418, 131965. <https://doi.org/10.1016/j.biortech.2024.131965>.
- Shi, S., Lin, Z., Zhou, J., Fan, X., Huang, Y., Zhou, J., 2022. Enhanced thermophilic denitrification performance and potential microbial mechanism in denitrifying granular sludge system. *Bioresour. Technol.* 344 (Pt A), 126190. <https://doi.org/10.1016/j.biortech.2021.126190>.
- Sun, H., Zhou, Q., Zhao, L., Wu, W., 2021. Enhanced simultaneous removal of nitrate and phosphate using novel solid carbon source/zero-valent iron composite. *J. Clean. Prod.* 289, 125757. <https://doi.org/10.1016/j.jclepro.2020.125757>.
- Tao, M., Kong, Y., Jing, Z., Jia, Q., Tao, Z., Li, Y.Y., 2022. Denitrification performance, bioelectricity generation and microbial response in microbial fuel cell - constructed wetland treating carbon constraint wastewater. *Bioresour. Technol.* 363, 127902. <https://doi.org/10.1016/j.biortech.2022.127902>.
- Valencia, R., Le, H., Zu, Y., Dittrich, T.M., Tsang, D.C.W., Datta, R., Sarkar, D., Mohanty, S.K., 2021. Nitrate removal uncertainty in stormwater control measures: is the design or climate a culprit? *Water Res.* 190, 116781. <https://doi.org/10.1016/j.watres.2020.116781>.
- Wang, C., He, T., Zhang, M., Zheng, C., Yang, L., Yang, L., 2024a. Review of the mechanisms involved in dissimilatory nitrate reduction to ammonium and the efficacies of these mechanisms in the environment. *Environ. Pollut.* 345, 123480. <https://doi.org/10.1016/j.envpol.2024.123480>.
- Wang, H., Chen, N., Feng, C., Deng, Y., 2021. Insights into heterotrophic denitrification diversity in wastewater treatment systems: progress and future prospects based on different carbon sources. *Sci. Total Environ.* 780, 146521. <https://doi.org/10.1016/j.scitotenv.2021.146521>.
- Wang, J., Li, X., Li, Y., Shi, Y., Xiao, H., Wang, L., Yin, W., Zhu, Z., Bian, H., Li, H., Shi, Z., Seybold, H., Kirchner, J.W., 2024b. Transport pathways of nitrate in stormwater runoff inferred from high-frequency sampling and stable water isotopes. *Environ. Sci. Technol.* 58 (38), 17026–17035. <https://doi.org/10.1021/acs.est.4c02495>.
- Wang, S., Ma, Y., Zhang, X., Yu, Y., Zhou, X., Shen, Z., 2022. Nitrogen transport and sources in urban stormwater with different rainfall characteristics. *Sci. Total Environ.* 837, 155902. <https://doi.org/10.1016/j.scitotenv.2022.155902>.
- Wang, S., Pi, Y., Song, Y., Jiang, Y., Zhou, L., Liu, W., Zhu, G., 2020. Hotspot of dissimilatory nitrate reduction to ammonium (DNRA) process in freshwater sediments of riparian zones. *Water Res.* 173, 115539. <https://doi.org/10.1016/j.watres.2020.115539>.
- Wang, Z., Song, B., Xu, L., He, Y., Chen, H., Zhang, A., Wang, Y., Tai, J., Zhang, R., Song, L., Xue, G., 2023. Organic carbon source excites extracellular polymeric substances to boost Fe⁰-mediated autotrophic denitrification in mixotrophic system. *Chemosphere* 337, 139352. <https://doi.org/10.1016/j.chemosphere.2023.139352>.
- Wang, Z., Yan, C., Wang, X., Xia, S., 2024c. Double-edged sword effects of sulfate reduction process in sulfur autotrophic denitrification system: accelerating nitrogen removal and promoting antibiotic resistance genes spread. *Bioresour. Technol.* 409, 131239. <https://doi.org/10.1016/j.biortech.2024.131239>.
- Weng, Z., Ma, H., Ma, J., Kong, Z., Shao, Z., Yuan, Y., Xu, Y., Ni, Q., Chai, H., 2022. Corn cob-pyrite bioretention system for enhanced dissolved nutrient treatment: carbon source release and mixotrophic denitrification. *Chemosphere* 306, 135534. <https://doi.org/10.1016/j.chemosphere.2022.135534>.
- Xiang, Z., Chen, X., Li, H., Zhu, B., Bai, J., Huang, X., 2025. Insight into enhanced adaptability of iron-carbon biofilter in treating low-carbon nitrogen mariculture wastewater for nitrogen removal and carbon reduction. *Bioresour. Technol.* 419, 132103. <https://doi.org/10.1016/j.biortech.2025.132103>.
- Xiong, R., Yu, X., Zhang, Y., Peng, Z., Yu, L., Cheng, L., Li, T., 2020. Comparison of agricultural wastes and synthetic macromolecules as solid carbon source in treating low carbon nitrogen wastewater. *Sci. Total Environ.* 739, 139885. <https://doi.org/10.1016/j.scitotenv.2020.139885>.
- Yadav, S., Ambastha, S., Pipil, H., Haritash, A.K., Reddy, K.R., 2025. Deciphering the sustainable stormwater management strategies for urban areas: a review. *Water Resour. Manag.* 39 (7), 2971–2991. <https://doi.org/10.1007/s11269-025-04222-6>.
- Yadav, S., Pipil, H., Haritash, A.K., Reddy, K.R., 2024. Fe(III)-modified bamboo biochar for the removal of phosphate from synthetic and field stormwater runoff. *Sustain. Water Resour. Manag.* 10, 140. <https://doi.org/10.1007/s40899-024-01123-1>.
- Yang, Y., Li, J., Kong, Z., Ma, J., Shen, Y., Ma, H., Yan, Y., Dan, K., Chai, H., 2024. A self-sustaining effect induced by iron sulfide generation and reuse in pyrite-woodchip mixotrophic bioretention systems: an experimental and modeling study. *Water Res.* 265, 122311. <https://doi.org/10.1016/j.watres.2024.122311>.
- Yang, Z., Sun, H., Zhou, Q., Zhao, L., Wu, W., 2020. Nitrogen removal performance in pilot-scale solid-phase denitrification systems using novel biodegradable blends for treatment of waste water treatment plants effluent. *Bioresour. Technol.* 305, 122994. <https://doi.org/10.1016/j.biortech.2020.122994>.
- You, G., Wang, C., Hou, J., Wang, P., Xu, Y., Miao, L., Liu, J., 2021. Effects of zero valent iron on nitrate removal in anaerobic bioreactor with various carbon-to-nitrate ratios: Bio-electrochemical properties, energy regulation strategies and biological response mechanisms. *Chem. Eng. J.* 419, 129646. <https://doi.org/10.1016/j.cej.2021.129646>.
- You, G., Wang, P., Hou, J., Wang, C., Xu, Y., Miao, L., Lv, B., Yang, Y., Zhang, F., 2017. The use of zero-valent iron (ZVI)-microbe technology for wastewater treatment with special attention to the factors influencing performance: a critical review. *Crit. Rev. Env. Sci. Tec.* 47 (10), 877–907. <https://doi.org/10.1080/10643389.2017.1334457>.
- Yuan, S., Zhong, Q., Zhang, H., Zhu, W., Wang, W., Li, M., Tang, X., Zhang, S., 2023. The enrichment of more functional microbes induced by the increasing hydraulic retention time accounts for the increment of autotrophic denitrification performance. *Environ. Res.* 236 (Pt 2), 116848. <https://doi.org/10.1016/j.envrres.2023.116848>.
- Zhang, C., Chen, H., Xue, G., 2025. Enhanced nitrogen removal from low C/N ratio wastewater by coordination of ternary electron donors of Fe⁰, carbon source and sulfur: focus on oxic/anoxic/oxic process. *Water Res.* 276, 123290. <https://doi.org/10.1016/j.watres.2025.123290>.
- Zhang, F., Ma, C., Huang, X., Liu, J., Lu, L., Peng, K., Li, S., 2021. Research progress in solid carbon source-based denitrification technologies for different target water bodies. *Sci. Total Environ.* 782, 146669. <https://doi.org/10.1016/j.scitotenv.2021.146669>.
- Zhang, L., Cui, Y., Dou, Q., Peng, Y., Yang, J., 2024. Sulfur-carbon loop enhanced efficient nitrogen removal mechanism from iron sulfide-mediated mixotrophic partial denitrification/anammox systems. *Bioresour. Technol.* 403, 130882. <https://doi.org/10.1016/j.biortech.2024.130882>.
- Zhang, Q., Ji, F., Xu, X., 2016. Effects of physicochemical properties of poly- ϵ -caprolactone on nitrate removal efficiency during solid-phase denitrification. *Chem. Eng. J.* 283, 604–613. <https://doi.org/10.1016/j.cej.2015.07.085>.
- Zhang, Q., Xu, X., Zhang, R., Shao, B., Fan, K., Zhao, L., Ji, X., Ren, N., Lee, D.J., Chen, C., 2022. The mixed/mixotrophic nitrogen removal for the effective and sustainable treatment of wastewater: from treatment process to microbial mechanism. *Water Res.* 226, 119269. <https://doi.org/10.1016/j.watres.2022.119269>.
- Zhao, Y., Wang, H., Dong, W., Chang, Y., Yan, G., Chu, Z., Ling, Y., Wang, Z., Fan, T., Li, C., 2020. Nitrogen removal and microbial community for the treatment of rural domestic sewage with low C/N ratio by A/O biofilter with Arundo donax as carbon source and filter media. *J. Water Process Eng.* 37, 101509. <https://doi.org/10.1016/j.jwpe.2020.101509>.
- Zhou, Q., Jia, L., Wu, W., Wu, W., 2022. Introducing PHBV and controlling the pyrite sizes achieved the pyrite-based mixotrophic denitrification under natural aerobic conditions: low sulfate production and functional microbe interaction. *J. Clean. Prod.* 366, 132986. <https://doi.org/10.1016/j.jclepro.2022.132986>.